Evaluation of Infiltration Discharge as a Strategy to Meet Effluent Temperature Limits

Ryan D. Stewart[1]; Daniel Moreno[2]; Christopher T. Gregory[3]; and John S. Selker[4]

Abstract: Recognizing that elevated stream temperatures can harm aquatic organisms, regulatory agencies have begun to enforce thermal total daily maximum load (TMDL) limits on wastewater discharges. Infiltration discharge, where treated wastewater is allowed to infiltrate into the soil and then percolate toward the stream or river, represents a potential method for meeting temperature requirements and for supplementing flow. This study combines observed and simulated temperature data to assess the efficacy of using infiltration discharge to meet effluent temperature limits. Observational data collected during operation of a 0.15-ha pilot-scale infiltration discharge system revealed the pattern of groundwater heating beneath the site by the wastewater, with the largest temperature increases occurring near the infiltration point. Numerical simulations used to examine the long-term groundwater response to operation of a 5.5-ha large-scale infiltration wetland system confirmed this trend and demonstrated how multiyear operation causes the heat to propagate outward from the infiltration point, primarily in the direction of the natural groundwater gradient. The numerical results also reveal how retention time can be an important factor in allowing heat to dissipate toward the surface and become removed from the system. To understand the ultimate fate of the wastewater heat, we formulated a set of nondimensional numbers computed using physical characteristics of the site and wastewater that compare hydraulic retention time with infiltration capacity and can be used to determine the potential of a site for infiltration discharge. We show the conditions under which infiltration discharge is a viable method for wastewater discharge within temperature limits. **DOI: 10.1061/JSWBAY.0000818.**

Introduction

As part of the Clean Water Act, regulatory agencies have implemented thermal loading restrictions on point source discharges such as those occurring from municipal wastewater treatment plants (USEPA 2006). In Oregon, the Department of Environmental Quality has started to enforce total daily maximum load (TMDL) limits on thermal loading for National Pollutant Discharge Elimination System (NPDES) permit holders.

Infiltration discharge represents a potential wastewater temperature mitigation strategy wherein treated wastewater is placed in shallow unlined wetlands and is then allowed to infiltrate the soil en route to nearby natural surface waters. Lancaster et al. (2005) used numerical simulations to investigate the use of a subsurface infiltration discharge system and determined that overall system performance was most affected by hydraulic conductivity and the distance between the injection point and the river. Although that study concluded that the use of a subsurface effluent discharge system could almost completely alleviate wastewater-induced temperature increases in the river, it was focused on a large river system where the wastewater discharge represents less than 1% of the total streamflow. On the other hand, many wastewater treatment plants, such as the City of Woodburn Publicly Owned Treatment Works (POTW), located in Woodburn, Oregon, discharge their effluent into relatively small streams and rivers. For example, the Pudding River, into which the POTW discharges, has an average August flow of 0.9 $m^3 s^{-1}$ (USGS 2010). The City of Woodburn is planning for an average plant loading rate of more than 0.2 $m^3 s^{-1}$ by the year 2030 (CH2MHill 2010), which could represent up to 25% of summer river flow. Thus, the results predicted by Lancaster et al. (2005) may not apply for such a system. To the authors' knowledge, no comparable study has been performed that focuses on the efficacy of infiltration discharge into smaller streams and rivers.

Heat, such as that originating from an infiltration discharge system, moves through the subsurface via two modes: convection (advection) and conduction. Convection refers to heat that is transported along with movement of the bulk fluid; conduction refers to the movement of heat in response to thermal gradients (i.e., from regions of high temperature to regions of low temperature). Moving fluids can also cause the thermal dispersion of heat due to local pore-scale differences in velocity (Anderson 2005). For solid materials, thermal conductivity can vary by a factor of approximately 35 (with organic matter on the low end and quartz on the high end; Duque et al. 2016); for porous media, the amount of water present also affects the magnitude of effective thermal conductivity (Anderson 2005). Nonetheless, thermal conductivity values in geologic materials have a much smaller range compared with hydraulic conductivity, which can vary by many orders of magnitude even in a single site or profile (Anderson 2005).

Thermal signatures in subsurface water are often used to discern interactions between stream water and groundwater. This includes studies of hyporheic exchange, where surface water infiltrates and moves through the subsurface for some distance before reemerging into the surface flow (e.g., Arrigoni et al. 2008; Khamis et al. 2015; Poole et al. 2008; Vandersteen et al. 2015);

[1]Assistant Professor, Dept. of Crop and Soil Environmental Science, Virginia Tech, 330 Smyth Hall, Blacksburg, VA 24061 (corresponding author). ORCID: http://orcid.org/0000-0002-9700-0351. E-mail: ryan.stewart@vt.edu

[2]Ph.D. Candidate, Dept. of Biological and Ecological Engineering, Oregon State Univ., 116 Gilmore Hall, Corvallis, OR 97333.

[3]Engineer, Montgomery & Associates, Calle Enrique Palacios 335, Of. 305 Miraflores, Lima 18, Peru.

[4]Professor, Dept. of Biological and Ecological Engineering, Oregon State Univ., 116 Gilmore Hall, Corvallis, OR 97333.

Note. This manuscript was submitted on September 29, 2015; approved on September 13, 2016; published online on November 8, 2016. Discussion period open until April 8, 2017; separate discussions must be submitted for individual papers. This paper is part of the ***Journal of Sustainable Water in the Built Environment***, © ASCE, ISSN 2379-6111.

it also includes assessment of gaining and losing stream reaches (e.g., Constantz 2008; Evans and Petts 1997; Silliman and Booth 1993; Taniguchi et al. 1999). The temperature profile of downwelling water often resembles that of the surface source, whereas up-welling typically shows a more buffered temperature signal (Briggs et al. 2014; Cranswick et al. 2014; Norman and Cardenas 2014; Taniguchi 1993). Depth of infiltration also influences the temperature characteristics of percolating water. Percolating water is typically shown to have an attenuated temperature signal with increasing depth from the source (Evans and Petts 1997; Silliman and Booth 1993), and larger vertical hydraulic gradients have been found to lead to dampened diel fluctuations (Malard et al. 2001). In general, water at depths of more than 1.5 m varies less than 1°C diurnally (Silliman and Booth 1993). However, a study in New Mexico showed little temperature gradient down to a depth of 3 m, likely because of the high permeability of the subsurface (Constantz and Thomas 1997). Seasonal temperature signals in groundwater are often evident down to a depth of ~20 m below the surface (Bense and Kooi 2004), whereas water below 20 m begins to warm because of the geothermal gradient; this gradient is estimated to range from 9 to 36°C km^{-1} (Domenico and Schwartz 1998). Deviations from these temperature patterns (e.g., caused by downward convection) can be used to estimate groundwater fluxes (Irvine et al. 2016).

This study combines observational data, focused on spatial and temporal temperature patterns that result from operation of a pilot-scale infiltration discharge system, with a large-scale numerical simulation to assess the feasibility of using infiltration discharge systems (Fig. 1). Using as an example a site located in Woodburn, Oregon, the study demonstrates how infiltration discharge systems can be used to translate treated wastewater from a heat source to a cooling feature of a temperature-limited stream. Finally, it presents and employs a set of nondimensional numbers that can be used to predict the fate and transport of heat carried in the wastewater and that can ultimately be used by municipalities and other treatment plant operations to assess the performance of such systems.

Methods

Site Description

The city of Woodburn, Oregon, is a historically agricultural town situated approximately 25 km northeast of Salem, Oregon, and 50 km south of Portland, Oregon. The city's wastewater operations are handled by the Woodburn POTW, positioned on a terrace above the historic floodplain of the Pudding River, a tributary of the Molalla River in the mid-Willamette River Basin. The lower Pudding River is confined from the deeper Willamette Aquifer material by a restrictive layer of Missoula Flood material known as Willamette Silt (Iverson 2002). Throughout the region Willamette Silt ranges between 6 and 30 m in thickness, whereas the Willamette Aquifer is between 12 and 60 m thick (Gannett and Caldwell 1998). The Willamette Silt layer in the floodplain adjacent to the POTW is primarily composed of Wapato-series and McBee-series silty clay loams.

In anticipation of new TMDL regulations, the City of Woodburn in 2004 commissioned a study on the viability of a large-scale infiltration discharge adjacent to the Pudding River. The POTW constructed a 56 × 26-m (0.15-ha) pilot-scale infiltration wetland in the river floodplain, approximately 250 m from the nearest point of the Pudding River. During the study period, the water level in the wetland was maintained at 0.3 m.

The pilot wetland was filled with tertiary-treated wastewater between May and September for the years 2006 and 2007. In 2008, the wetland was only intermittently filled because of rodent damage. In 2009, the wetland was again filled between May and September. In this final year, the wetland and surrounding floodplain were extensively monitored in order to evaluate the potential of infiltration discharge for meeting effluent temperature limits. These observational data were used to calibrate a three-dimensional (3D) groundwater model for the site using the *HYDRUS-2D/3D* software package (Simunek and Sejna 2011). The model was then used to simulate the operation of a full-size (5.5-ha) infiltration discharge system over a period of 11 years in order to assess the impacts on surrounding groundwater.

Groundwater Monitoring

The site was equipped with one monitoring well at 22-m depth (MW8), three monitoring wells at 10-m depth (MW5, MW6, and MW7), six piezometers at 4-m depth (P2-P7), and one piezometer at 1.5-m depth (P1; Fig. 2). Each piezometer and monitoring well was outfitted with a Hobo U20 series data-logging pressure transducer (Onset, Massachusetts) installed approximately 0.5 m from the well bottom. The pressure transducers were set to record pressure and temperature readings at 15-min intervals. The temperature calibrations of the loggers were confirmed by placing them for approximately 30 min in an ice bath, with the loggers set to record every 5 sec. To get water table elevations, the pressure data were corrected using hourly barometric pressure from the National Climatic Data Center (NCDC) weather station data at the Aurora Airport (UAO), located approximately 11 km from the site.

Numerical Simulations

To simulate the long-term groundwater temperature resulting from operation of a 5.5-ha infiltration wetland, a 3D model of the floodplain was created (Stewart et al. 2015) using the *HYDRUS 2D/3D* software package. The model was created with dimensions of 750 m (width) × 1,500 m (length) × 32–40 m (height). Four soil layers were modeled; the hydraulic properties of each one are listed in Table 1. Default thermal properties were used (Chung and Horton 1987), with the upper soil layer being modeled as a clay, the second soil layer being modeled as a loam, and the lower two layers being modeled as a sand. One percent organic matter content (by volume) was assumed for the uppermost layer.

Between May 1 and September 30 of each year, the portion of the upper boundary corresponding to the infiltration wetland was set with a constant head of 0.25 m and a temperature of 22°C using the Direchlet (first-type) heat transport boundary condition. The temperature for the wetland nodes was allowed to vary by ±2°C

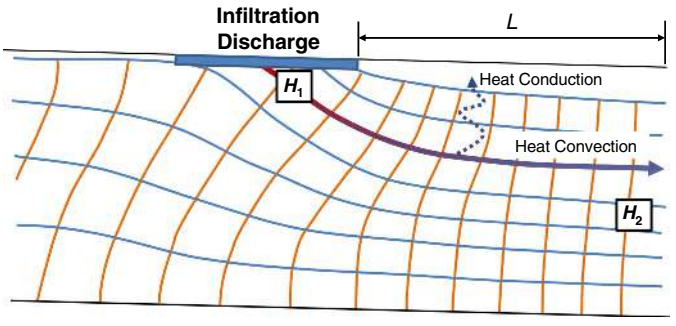

Fig. 1. Two-dimensional (vertical) schematic of an infiltration discharge system, with orange lines representing equipotential contours (e.g., H_1, H_2) and blue lines representing streamlines

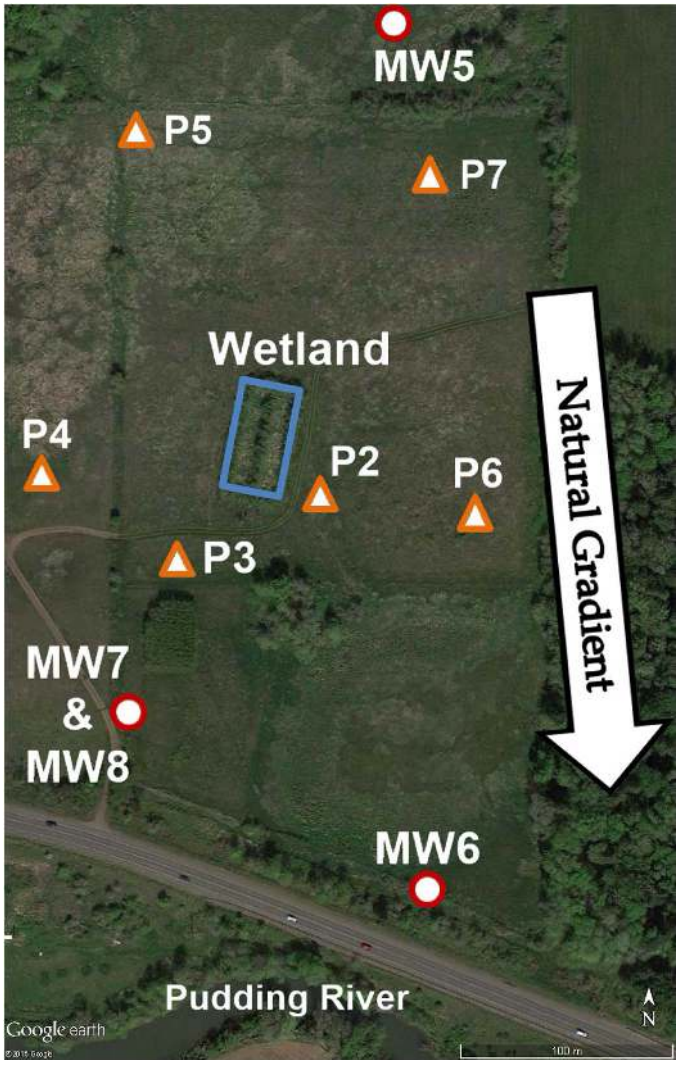

Fig. 2. Site map showing locations of the wetland, piezometers, monitoring wells, and Pudding River (map data © 2016 Google)

over the course of each day, with the maximum temperature (24°C) occurring at 1 p.m. The remainder of the upper boundary was described with the atmospheric boundary condition, using UAO meteorological data from May 1, 1999, to April 30, 2010. Between October 1 and April 30 of each year, the entire upper boundary was modeled using atmospheric boundary conditions. The bottom boundary was modeled with a no-flux condition. The side boundaries had constant head conditions that simulated a water table occurring 2–3 m below the soil surface.

Because of model instability when the water table rose to the model surface, large precipitation events were reduced in magnitude until the model became stable; the clipped precipitation

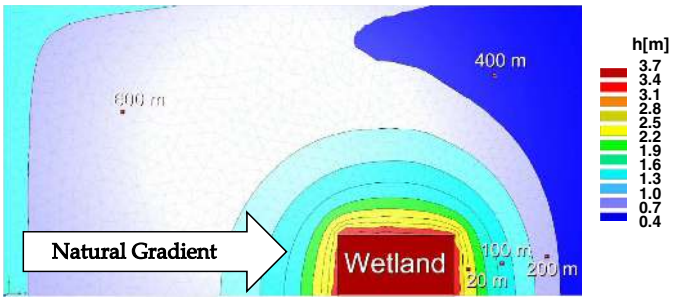

Fig. 3. Overhead view of 3D model created using *HYDRUS-3D*, with infiltration wetland and observation nodes highlighted

amounts were attributed to surface runoff. As an example, during the first winter (October 1, 1999–April 30, 2000), 65 daily precipitation records were clipped, for a total removal of 30 cm of precipitation (out of a total precipitation of 80 cm). This 37% runoff rate was typical of the amount of precipitation that needed to be removed to ensure model stability.

To access the long-term impact caused by operating a large-scale infiltration wetland, temperature results were compiled from arrays of observation nodes corresponding to five locations around the floodplain: (1) 20 m down-gradient from the wetland; (2) 100 m down-gradient from the wetland (equivalent to the closest point of the Pudding River); (3) 200 m down-gradient from the wetland; (4) 400 m from the side of the wetland; and (5) 600 m up-gradient from the wetland (Fig. 3). Temperature measurements were taken from four depths at each location (3.5, 5.2, 6.9, and 8.6 m below the surface). Relative temperature ($\bar{T}$) increases caused by heat from the wetland water were quantified as

$$\bar{T} = \frac{T - T_{\text{ambient}}}{T_i - T_{\text{ambient}}} \tag{1}$$

where T = temperature of percolating water that originated at the infiltration point (at any given point along its flow path); T_i = initial water temperature; and T_{ambient} = temperature of the ambient groundwater.

T_{ambient} was considered to be the temperature of the water at the corresponding depth at the 600-m (up-gradient) position.

Results and Discussion

Observed Groundwater Temperature

Groundwater temperatures observed in the 10- and 22-m deep monitoring wells were nearly constant over a one-year period (Fig. 4). The clustered wells MW7 and MW8 showed elevated water temperature compared with MW5 and MW6, with an overall difference of approximately 1.5°C. Pressure head data collected in the wells showed an upward gradient between MW7 and MW8 for

Table 1. Soil Hydraulic and Thermal Properties Used in the *HYDRUS-3D* Numerical Model

Model layer	Depth (m)	α (m^{-1})	n	θ_s	θ_r	K_{vertical} ($m\,d^{-1}$)	$K_{\text{horizontal}}$ ($m\,d^{-1}$)	λ_e ($W\,m^{-1}\,K^{-1}$)
Layer 1	0–1.5	0.910	1.4827	0.4461	0.0708	0.778	7.130	1.06
Layer 2	1.5–4.5	1.565	1.3371	0.4565	0.0886	0.778	7.130	1.46
Layer 3	4.5–9	2.740	1.4092	0.3841	0.0501	0.323	0.323	2.35
Layer 4	9–40	3.450	2.4475	0.3788	0.0500	2.962	2.962	2.34

Note: The effective thermal conductivity λ_e represents the value calculated in the absence of flow and does not include macrodispersivity due to fluid flow.

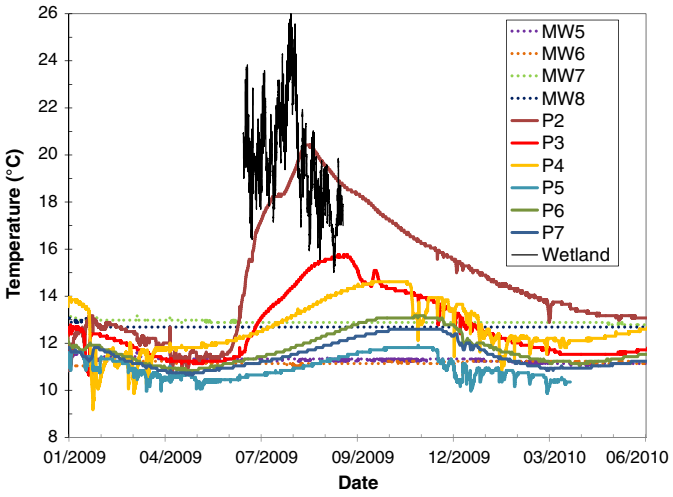

Fig. 4. Groundwater and wetland temperatures for a 1.5-year period beginning January 1, 2009

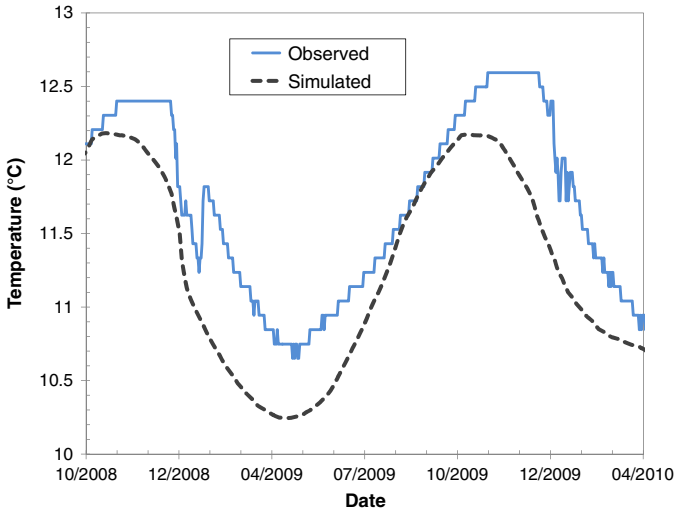

Fig. 5. Observed temperature at 4-m depth as observed in Piezometer 7 and predicted by *HYDRUS-3D*

much of the year (Stewart 2010), which could indicate that deeper groundwater was upwelling at that location. Another possibility is that elevated temperatures in MW7 and MW8 were caused by heat arriving from the pilot wetland, as the wetland was filled with warm wastewater for at least a portion of the three previous summers.

In comparison with the deep monitoring wells, temperatures in the shallow piezometers showed much greater variability. In 2009, the wetland was first filled with wastewater on April 15, and after being filled and drained a number of times for maintenance began regular operation on approximately May 15. The two piezometers closest to the wetland, P2 and P3, began to increase in temperature within a month of the wetland being regularly operated. The temperatures in those two piezometers also peaked at an earlier time than the more distant piezometers.

Ambient Groundwater Temperature

As a validation of the numerical model, the observed and simulated temperatures of shallow ambient groundwater (i.e., groundwater not influenced by the infiltration wetland) were compared over the period of October 1, 2008–April 1, 2010 (Fig. 5). The observed data came from Piezometer P7, which was located approximately 140 m up-gradient from the pilot wetland and was shown by chemical analyses to be unaffected by wetland operation (Stewart et al. 2015). The modeled data were compiled from the observation node located 600 m up-gradient from the wetland. Both the observed and simulated data were taken from a depth of approximately 4 m.

The model appeared to capture the amplitude and phase of the annual temperature signal, although the predicted temperatures were at times slightly colder than shown by the observations (up to 0.5°C). Nonetheless, the numerical model appears to simulate the gross temporal behavior of the thermal regime of the shallow floodplain groundwater system.

Long-Term Groundwater Temperature

The numerical model was next used to determine the temperature dynamics of the infiltrated wastewater and to examine how the heat of the wastewater moved through the groundwater. Seasonal temperature profiles (corresponding to October 1, January 1, and May 1) were compiled at three distances from the wetland (20, 100, and 400 m) during the first and eighth year of wetland operation. Even during the first year of operation, it is clear that the wastewater heat was influencing seasonal temperature at 20 m, as the profile was both warmer and more variable than at the 100- and 400-m distances [Fig. 6(a)]. By Year 8, the wastewater heat had reached and was influencing the temperature profile at the 100-m location [Fig. 6(b)]; however, this location showed considerably less warming than the 20-m distance. This suggests that water at this location is being influenced by both the wetland water and the ambient groundwater.

By simulating 11 years of infiltration discharge, the authors were able to determine when various portions of the shallow groundwater approached "steady-state" temperature profiles. Each location/depth was considered to reach steady-state conditions when the temperature first came within 0.1°C of any subsequent maximum annual value observed at that node. Based on the 3.5- and 5.2-m deep nodes, the 20-m distance reached a steady-state temperature profile after only four years (Fig. 7). The 100-m distance reached steady-state conditions after six years, and the 200-m distance attained a steady-state temperature profile after eight years. The 6.9- and 8.6-m depths followed a similar pattern, although in certain locations it did not reach steady-state conditions until one year after the upper two nodes. A power law function fit the data well (Fig. 7; $y = 1.35 \times 0.33$, $R^2 = 0.99$), providing a simple first estimate of the relative time required to achieve steady-state conditions as a function of distance from the infiltration point.

The *HYDRUS-3D* simulations were also used to determine maximum relative water temperature [$\bar{T}$; Eq. (1)] for the observation nodes located at $L = 20$, 100, 200, and 400 m. In this analysis, the initial water temperature T_i was set equal to 22°C, and the ambient groundwater temperature T_{ambient} (determined using the simulation results from the 600-m location) was found to be 12.4°C at the 3.5-m depth, 12.0°C at the 5.2-m depth, 11.5°C at the 6.9-m depth, and 11.7°C at the 8.6-m depth. The percolating water temperature (T) was taken to be the maximum water temperature experienced at each node during the simulation. Note that a relative temperature value of 1 indicates that the discharge to the stream is equal to the temperature of the wetland water, whereas a value of 0 indicates discharge at the temperature of the ambient groundwater.

Based on the simulation results (Fig. 8), the wetland operation increased the relative temperature at the 20-, 100-, and 200-m

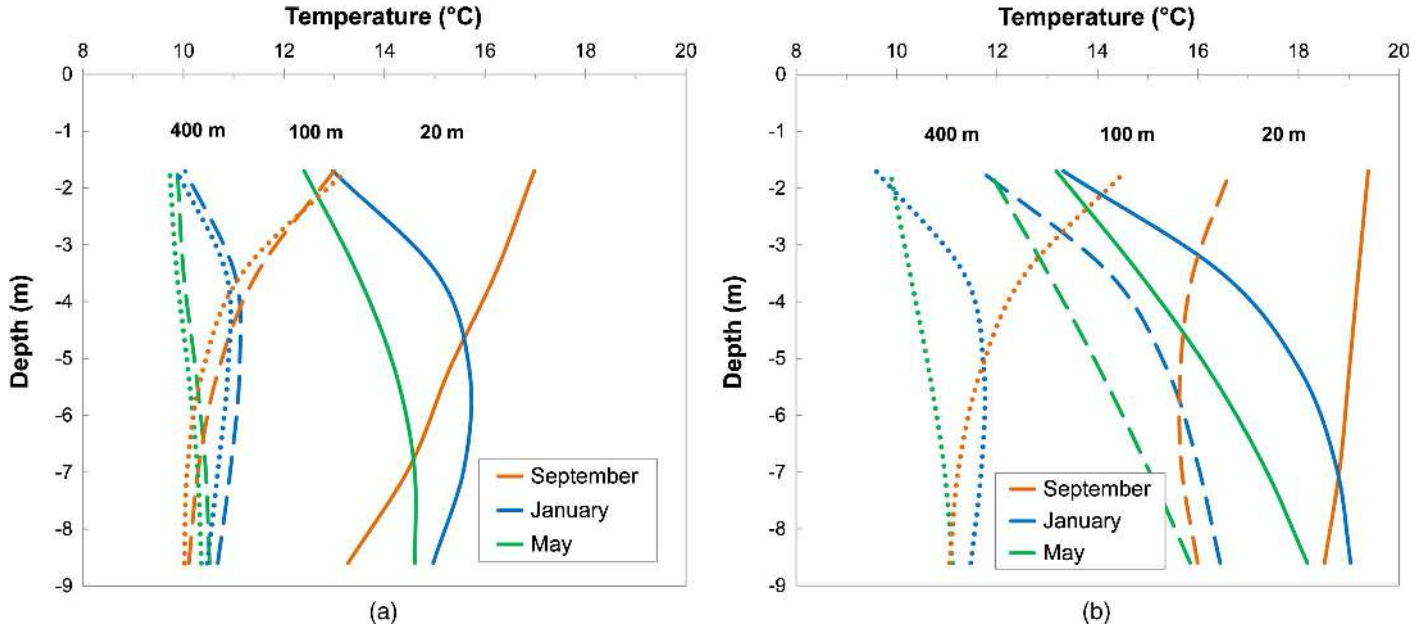

Fig. 6. Modeled temperature profile, with depth, for the 20-, 100-, and 400-m distances from wetland from (a) Year 1; (b) Year 8 (both years span May 1–April 30); solid lines represent the 20-m distance, dashed lines represent the 100-m distance, and dotted lines represent the 400-m distance

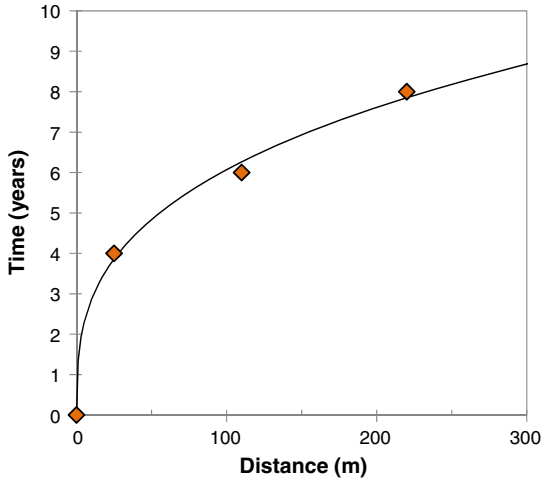

Fig. 7. Modeled number of years required to reach steady-state temperature conditions as a function of distance from the infiltration wetland

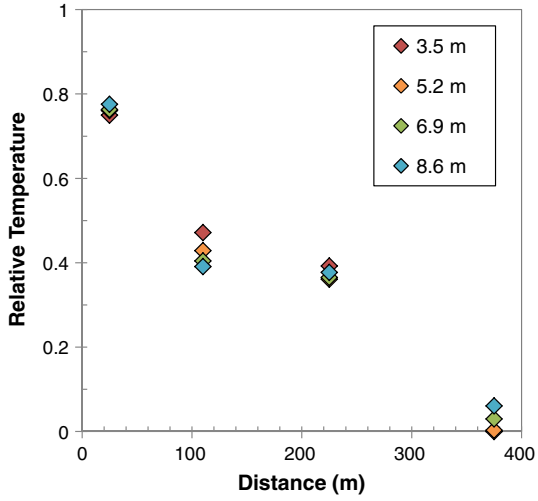

Fig. 8. Relative subsurface water temperature (1 = wetland water temperature; 0 = ambient water temperature) at four depths and four distances from the wetland

locations, with the 20-m distance having a relative temperature of approximately 0.75. The 100- and 200-m distances both showed relative temperatures of approximately 0.40, whereas the 400-m distance showed minimal or no temperature increase due to heat from the wetland. Moreover, at each distance all four depths (3.5, 5.2, 6.9, and 8.6 m) showed similar relative temperatures, suggesting that the wetland heat was becoming distributed throughout the shallow subsurface. It should be noted, however, that the shallower depths typically reached their maximum temperatures earlier than the deeper depths. For example, as seen in Fig. 6, the 8.6-m depth reached its maximum temperature 1–3 months later than the 3.5-m depth. This result suggests that the atmospheric/surface temperatures were affecting the shallow groundwater temperatures, as is typically observed in the surficial subsurface zone (e.g., Parsons 1970).

The simulation also showed that elevated temperatures were predicted to occur at greater distances from the wetland in the down-gradient direction compared with the up-gradient and cross-gradient directions (Fig. 9), which demonstrates the impact of groundwater movement on temperatures. Taken together, these findings indicate that temperature effects due to infiltration discharge of heated wastewater are greatest in the immediate vicinity of the infiltration point and then decrease with distance, likely because of heat exchange with the soil surface and then with the atmosphere. In other words, greater distances from the wetland are associated with longer hydraulic retention times, allowing more opportunity for the wetland heat to be removed from the system via atmospheric removal. Thus, when designing such systems, the direction and magnitude of the natural groundwater gradient should be taken into consideration because that ultimately influences the rate and extent of heat convection through the subsurface and heat exchange with the surface.

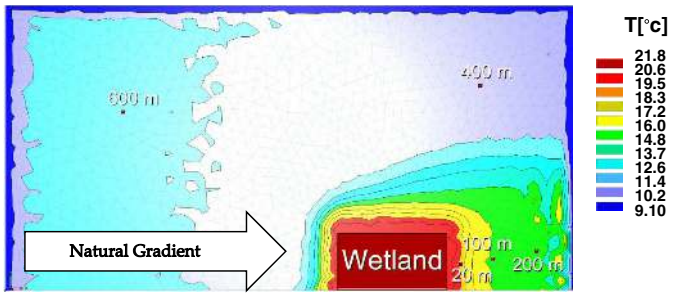

Fig. 9. *HYDRUS-3D*-modeled temperature distribution at 8.6-m depth after 11 years of infiltration discharge system operation

Design Considerations for Infiltration Discharge Systems

The simulated and observational data suggest that infiltration discharge systems could be designed with sufficient hydraulic retention time to buffer peak wastewater temperatures and, in some cases, allow the wastewater to come to thermal equilibrium with the atmosphere. Systems that have soils with low permeability or have large distances between the infiltration wetland and the river may possess sufficient hydraulic retention time to fully cool the water. On the other hand, soils with low permeability may severely limit the amount of water that can be discharged, making an infiltration discharge system an impractical solution. Likewise, physical, legal, and financial constraints often limit the practical distance between the injection wetland and the river and limit the size of the system. Thus, the feasibility of an infiltration discharge system depends on many variables, including hydraulic retention time, soil permeability, and infiltration wetland location and area.

In an attempt to simplify the initial feasibility determination process, the authors propose a set of nondimensional numbers based on quantifiable site and design parameters. The first nondimensional number, R, is a relationship of the hydraulic retention time of a system ($\tau_{\text{retention}}$) compared with the minimum recommended retention time (τ_{min}), and is derived using Darcy's law assuming horizontal water movement:

$$R = \frac{\tau_{\text{min}}}{\tau_{\text{retention}}} = \frac{\tau_{\text{min}}}{L/v} = \frac{\tau_{\text{min}} K_s \nabla H}{nL} \approx \frac{\tau_{\text{min}} K_s \Delta H}{nL^2} \qquad (2)$$

where v = water velocity; n = effective porosity of the media (or volumetric water content in the case of unsaturated media); K_s = hydraulic conductivity of the media in the direction of the water flow (e.g., horizontal); ∇H = gradient in hydraulic head; and ΔH = change in hydraulic head that occurs over the distance L (Fig. 1).

The variable L represents the straight-line distance rather than the actual distance traveled by any parcel of water.

The minimum recommended retention time (τ_{min}) varies based on design and permit requirements, but in general should at least be long enough to ensure that peak temperatures arrive at the stream after the critical summer period (i.e., 3–6 months). An R value much less than 1 signifies that the system has adequate retention time.

The second nondimensional number, J, relates the desired volumetric infiltration rate to the infiltration capacity of the site:

$$J = \frac{Q_{\text{load}}}{Q_{\text{infiltration}}} = \frac{Q_{\text{load}}}{K_s A \nabla H} \approx \frac{Q_{\text{load}} L}{K_s A \Delta \text{H}} \qquad (3)$$

where Q_{load} = desired volumetric loading rate $[L^3\,T^{-1}]$; and A = area of the infiltration system. Infiltration discharge systems can cause two different water table responses. In the first case, the water table rises and becomes hydraulically connected to the infiltration basin (e.g., Petrides et al. 2015; Stewart et al. 2015); in the second case, the groundwater mound remains separated from the basin by an unsaturated zone (e.g., Rastogi and Pandey 1998). Eqs. (2) and (3) were formulated assuming that the water table is directly connected to the infiltration basin and therefore may need to be modified if an unsaturated zone exists above the groundwater mound. Likewise, Eqs. (2) and (3) do not account for any clogging layers (Bouwer and Rice 1989) or other heterogeneity in soil properties that may exist.

The City of Woodburn proposed constructing a full-scale infiltration wetland system to infiltrate up to 0.2 $m^3\,s^{-1}$ ($Q_{\text{load}} = 1.78 \times 10^4$ $m^3\,d^{-1}$). The city has 5.5 ha of available land on which to create the infiltration wetlands, located approximately 200 m from the Pudding River. Thus, by using the estimated horizontal hydraulic conductivity of the floodplain ($K_s = 7.13$ $m\,d^{-1}$; Stewart et al. 2015), and assuming $\Delta H = 3$ m (Fig. 3), Eq. (3) yields a value of $J = 3.0$. Because $J > 1$, the City of Woodburn will not likely be able to infiltrate as much wastewater as is desired without altering the system design (such as increasing the infiltration area). The predicted $Q_{\text{infiltration}}$ value ($Q_{\text{infiltration}} = 5.8 \times 10^3$ $m^3\,d^{-1}$) closely matches the volumetric infiltration fluxes predicted by *HYDRUS-3D* for Years 1 and 11 (Fig. 10). This suggests that Eq. (3) may be an adequate method to predict the infiltration capacity of a site.

By plotting R and J together, the authors created a design chart that can be used to assess the feasibility of a given location and/or infiltration discharge system design (Fig. 11). The sample space has been divided into four regions to allow for easy interpretation of the chart. Region 1 (where R and J are both less than 1) signifies that the design is feasible because the system is predicted to have sufficient retention time and infiltration capacity. Region 2 (where R is between 1 and 10 and J is less than 10) and Region 3 (where J is between 1 and 10 and R is less than 10) indicate where the design is likely to be feasible, but should be evaluated to ensure it has either sufficient hydraulic retention time (Region 2) or infiltration capacity (Region 3). Note that a value of 10 was selected as the upper limit of these regions to allow for one order of magnitude of uncertainty in the predictions of R and J because those equations do not account for effects such as 3D infiltration from the source or

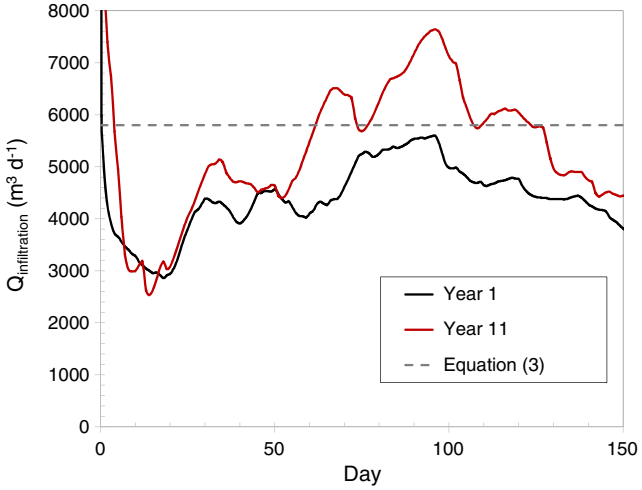

Fig. 10. Volumetric infiltration flux predicted by the *HYDRUS-3D* model for the 1st and 11th year of wetland operation, compared with $Q_{\text{infiltration}}$ predicted by Eq. (3) using site- and design-specific parameters

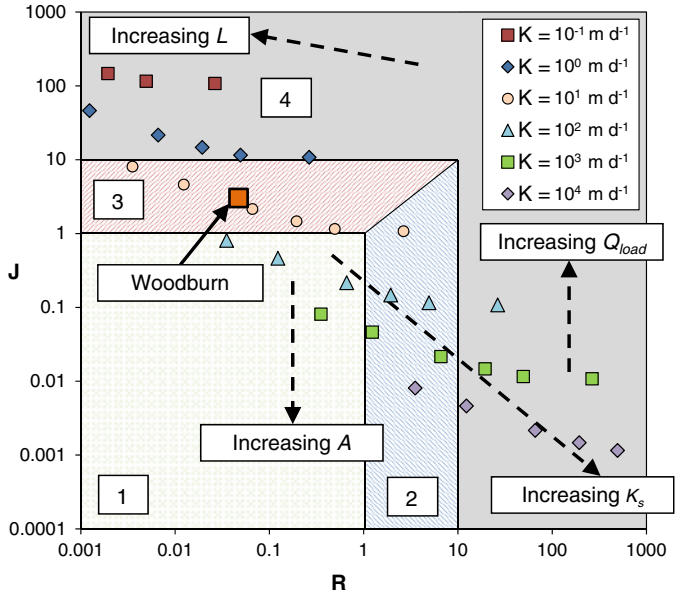

Fig. 11. Plot of dimensionless numbers R (retention time constant) versus J (infiltration rate constant) that can be used to assess site feasibility for infiltration discharge; the four regions are (1) feasible; (2) possible retention-time constraints; (3) possible infiltration constraints; and (4) not feasible; the points for each data series from left to right indicate values of $L = 1{,}000$, 500, 200, 100, 50, and 10 m; the "Woodburn" point shows the predicted location of a 5.5-ha infiltration wetland located 200 m from the river with Q_{load} of $7,570$ m^3 d^{-1}

thermal dissipation through the soil surface. Region 4 (where R and/or J are greater than 10) indicates that infiltration discharge would likely be infeasible based on the proposed site and/or design. In general it can be assumed that moderate hydraulic conductivity (K_s) values may allow for feasible infiltration discharge systems, whereas K_s values on either extreme will make it difficult to design an infiltration discharge system with satisfactory performance.

Conclusion

A combination of observational data and numerical simulations allowed assessment of the thermal influence of an infiltration discharge system on nearby groundwater. By simulating multiple years of system operation, it was observed that shallow groundwater temperatures went through a transition (warming) phase before reaching new steady-state conditions. The rate and total amount of warming depended on the proximity to the discharge point, with locations in the immediate vicinity of the infiltration point showing warmer temperatures and faster transitions to the new thermal regime. The overall time to steady-state temperatures was found to be well described as a power law function of distance. These trends are likely driven by retention time: the longer the heated wastewater remains in the subsurface, the greater opportunity it has to dissipate its heat. This is an important consideration when designing infiltration discharge systems because infiltration points located in close proximity to the receiving water body—where wastewater treatment plants are often located—may not impart sufficient thermal benefit.

The permeability of the soil represents another parameter with conflicting effects on overall system performance. Specifically, higher hydraulic conductivity values imply that the system will be able to infiltrate greater quantities of water and can help such systems achieve economy of scale. However, higher permeabilities also result in reduced retention time and less opportunity for heat to be dissipated in the subsurface. Recognizing that system optimization is a complex process that depends on system demands, local geology, and political/economic constraints, the two sets of nondimensional numbers proposed in this study can help site designers rapidly evaluate the potential of any given location for infiltration discharge. In particular, the infiltration discharge design chart developed in this study (Fig. 11) should allow for wastewater agencies and/or engineering firms to forego extensive modeling and/or pilot-scale assessment efforts.

The results of this study imply that wastewater treatment facilities faced with discharge temperature limits may be able to construct infiltration discharge systems with sufficient hydraulic retention time to spread out and possibly cool the wastewater heat. Depending on the specifics of an individual facility's permit, this can be used to ensure compliance with temperature TMDLs. Altogether, infiltration discharge appears to represent a feasible and potentially economical method by which certain wastewater treatment plants can comply with environmental regulations and preserve the quality of natural waterways.

Acknowledgments

The authors offer their gratitude to Jason Smesrud, the project manager representing CH2M Hill, and Curtis Stultz, the City of Woodburn POTW manager. They also acknowledge Kyle Chambers for his collaboration during the project. This research would not have been possible without the POTW staff, especially the efforts of Mike Arellano, Ramon Garcia, and Jordan Garner. Finally, the authors express special thanks to Dr. Roy Haggerty of Oregon State University for providing ideas and discussions regarding the dimensionless representation of the results that greatly benefited to this work.

References

Anderson, M. P. (2005). "Heat as a ground water tracer." *Ground Water*, 43(6), 951–968.

Arrigoni, A. S., Poole, G. C., Mertes, L. A. K., O'Daniel, S. J., Woessner, W. W., and Thomas, S. A. (2008). "Buffered, lagged, or cooled? Disentangling hyporheic influences on temperature cycles in stream channels." *Water Resour. Res.*, 44(9), W09418.

Bense, V., and Kooi, H. (2004). "Temporal and spatial variations of shallow subsurface temperature as a record of lateral variations in groundwater flow." *J. Geophys. Res.*, 109(B4), 1–13.

Bouwer, H., and Rice, R. C. (1989). "Effect of water depth in groundwater recharge basins on infiltration." *J. Irrig. Drain. Eng.*, 10.1061/(ASCE)0733-9437(1989)115:4(556), 556–567.

Briggs, M. A., Lautz, L. K., Buckley, S. F., and Lane, J. W. (2014). "Practical limitations on the use of diurnal temperature signals to quantify groundwater upwelling." *J. Hydrol.*, 519, 1739–1751.

CH2MHill. (2010). "Wastewater facilities plan. Volume 1: Wastewater treatment." Woodburn, OR.

Chung, S. O., and Horton, R. (1987). "Soil heat and water flow with a partial surface mulch." *Water Resour. Res.*, 23(12), 2175–2186.

Constantz, J. (2008). "Heat as a tracer to determine streambed water exchanges." *Water Resour. Res.*, 44(4), W00D10.

Constantz, J., and Thomas, C. L. (1997). "Stream bed temperature profiles as indicators of percolation characteristics beneath arroyos in the Middle Rio Grande Basin, USA." *Hydrol. Processes*, 11(12), 1621–1634.

Cranswick, R. H., Cook, P. G., Shanafield, M., and Lamontagne, S. (2014). "The vertical variability of hyporheic fluxes inferred from riverbed temperature data." *Water Resour. Res.*, 50(5), 3994–4010.

Domenico, P. A., and Schwartz, F. W. (1998). *Physical and chemical hydrogeology*, 2nd Ed., Wiley, New York, 506.

Duque, C., Müller, S., Sebok, E., Haider, K., and Engesgaard, P. (2016). "Estimating groundwater discharge to surface waters using heat as a tracer in low flux environments: The role of thermal conductivity." *Hydrol. Processes*, 30(3), 383–395.

Evans, E., and Petts, G. E. (1997). "Hyporheic temperature patterns within riffles." *Hydrol. Sci. J.*, 42(2), 199–213.

Gannett, M. W., and Caldwell, R. R. (1998). "Geologic framework of the Willamette Lowland aquifer system, Oregon and Washington." U.S. Geological Survey, Washington, DC.

Irvine, D. J., Cartwright, I., Post, V. E., Simmons, C. T., and Banks, E. W. (2016). "Uncertainties in vertical groundwater fluxes from 1-D steady state heat transport analyses caused by heterogeneity, multidimensional flow, and climate change." *Water Resour. Res.*, 52(2), 813–826.

Iverson, J. (2002). "Investigation of the hydraulic, physical, and chemical buffering capacity of Missoula flood deposits for water quality and supply in the Willamette Valley of Oregon." M.S. thesis, Oregon State Univ., Corvallis, OR.

Khamis, K., Brown, L. E., Milner, A. M., and Hannah, D. M. (2015). "Heat exchange processes and thermal dynamics of a glacier-fed alpine stream." *Hydrol. Processes*, 29(15), 3306–3317.

Lancaster, S., Haggerty, R., Gregory, S., Farthing, K. T., and Biorn-Hansen, S. (2005). "Investigation of the temperature impact of hyporheic flow: Using groundwater and heat flow modeling and GIS analyses to evaluate temperature mitigation strategies on the Willamette River, Oregon." Oregon Dept. of Environmental Quality, Corvallis, OR.

Malard, F., Mangin, A., Uehlinger, U., and Ward, J. V. (2001). "Thermal heterogeneity in the hyporheic zone of a glacial floodplain." *Can. J. Fish. Aquat. Sci.*, 58(7), 1319–1335.

Norman, F. A., and Cardenas, M. B. (2014). "Heat transport in hyporheic zones due to bedforms: An experimental study." *Water Resour. Res.*, 50(4), 3568–3582.

Parsons, M. L. 1970. "Groundwater thermal regime in a glacial complex." *Water Resour. Res.*, 6(6), 1701–1720.

Petrides, A., Stewart, R. D., Bower, R., Cuenca, R., and Wolcott, B. (2015). "Case study: Scaling recharge rates from pilot projects of managed artificial aquifer recharge in the Walla Walla Basin, Oregon." *J. Hydrolog. Eng.*, 10.1061/(ASCE)HE.1943-5584.0001102, 05014028.

Poole, G. C., et al. (2008). "Hydrologic spiralling: The role of multiple interactive flow paths in stream ecosystems." *River Res. Appl.*, 24(7), 1018–1031.

Rastogi, A. K., and Pandey, S. N. (1998). "Modeling of artificial recharge basins of different shapes and effect on underlying aquifer system." *J. Hydrolog. Eng.*, 10.1061/(ASCE)1084-0699(1998)3:1(62), 62–68.

Silliman, S., and Booth, D. (1993). "Analysis of time-series measurements of sediment temperature for identification of gaining versus losing portions of Juday Creek, Indiana." *J. Hydrol.*, 146, 131–148.

Simunek, J., and Sejna, M. (2011). "The HYDRUS software package for simulating the two-and three-dimensional movement of water, heat, and multiple solutes in variably-saturated media." PC-Progress, Prague, Czech Republic.

Stewart, R. D. (2010). "Infiltration and temperature characterization of a wastewater hyporheic discharge system." M.S. thesis, Oregon State Univ., Corvallis, OR.

Stewart, R. D., Moreno, D., and Selker, J. S. (2015). "Quantification and scaling of infiltration and percolation from a constructed wetland." *J. Hydrolog. Eng.*, 10.1061/(ASCE)HE.1943-5584.0001164, 04015007.

Taniguchi, M. (1993). "Evaluation of vertical groundwater fluxes and thermal properties of aquifers based on transient temperature-depth profiles." *Water Resour. Res.*, 29(7), 2021–2026.

Taniguchi, M., et al. (1999). "Disturbances of temperature-depth profiles due to surface climate change and subsurface water flow. 1: An effect of linear increase in surface temperature caused by global warming and urbanization in the Tokyo metropolitan area, Japan." *Water Resour. Res.*, 35(5), 1507–1517.

USEPA (U.S. Environmental Protection Agency). (2006). "2006 section 303(d) list fact sheet for Oregon—Total maximum daily loads." ⟨http://oaspub.epa.gov/tmdl/state_rept.control?p_state=OR&p_cycle=2006⟩ (Feb. 10, 2010).

USGS (U.S. Geological Survey). (2010). "Daily data from USGS Streamgage 14201340." ⟨http://waterdata.usgs.gov/or/nwis/uv/?site_no=14201340&PARAmeter_cd=00065,00060⟩. (Jan. 10, 2010).

Vandersteen, G., Schneidewind, U., Anibas, C., Schmidt, C., Seuntjens, P., and Batelaan, O. (2015). "Determining groundwater-surface water exchange from temperature-time series: Combining a local polynomial method with a maximum likelihood estimator." *Water Resour. Res.*, 51(2), 922–939.